

Supplementary Information for Chemical Informatics and Target Identification in a Zebrafish Phenotypic Screen

Christian Laggner,^{1†} David Kokel,^{2,3†} Vincent Setola,^{4†} Alexandra Tolia,⁵ Henry Lin,¹
John J. Irwin,¹ Michael J. Keiser,¹ Chung Yan J. Cheung,^{2,3} Daniel L. Minor, Jr.⁵ Bryan L.
Roth,^{4*} Randall T. Peterson^{2,3*} & Brian K. Shoichet^{1*}

¹Department of Pharmaceutical Chemistry, University of California, San Francisco, California, USA. ²Cardiovascular Research Center and Division of Cardiology, Department of Medicine, Massachusetts General Hospital, Harvard Medical School, Charlestown, Massachusetts, USA. ³Broad Institute, Cambridge, Massachusetts, USA. ⁴Department of Pharmacology and National Institute of Mental Health Psychoactive Drug Screening Program, University of North Carolina Chapel Hill School of Medicine, Chapel Hill, North Carolina, USA. ⁵Cardiovascular Research Institute, Departments of Biochemistry and Biophysics, and Cellular and Molecular Pharmacology, University of California, San Francisco, California, USA.

† These authors contributed equally

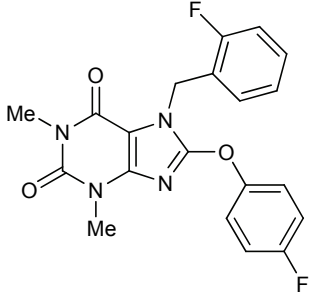
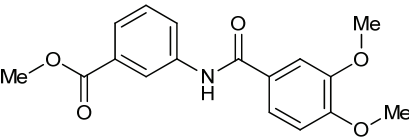
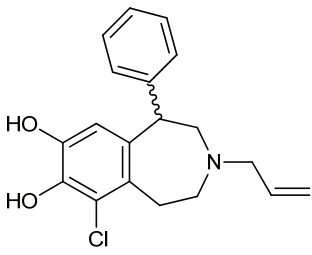
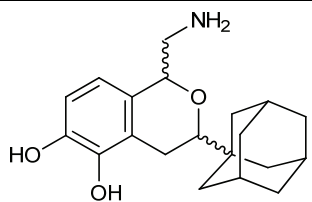
Bryan Roth: *bryan_roth@med.unc.edu*, phone: 919-966-7539, fax: 919-843-5788

Randall Peterson: *peterson@cvrc.mgh.harvard.edu*, phone: 617-724-9569, fax: 617-726-5806

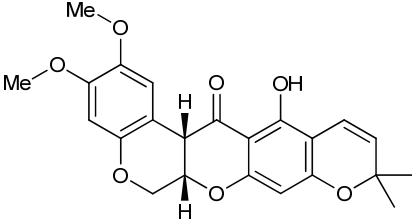
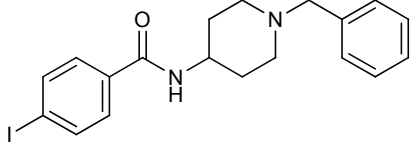
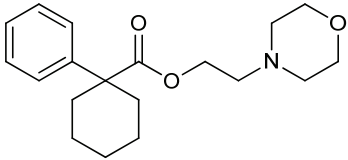
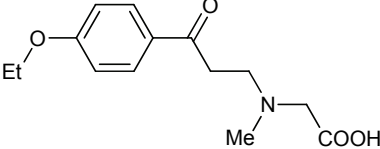
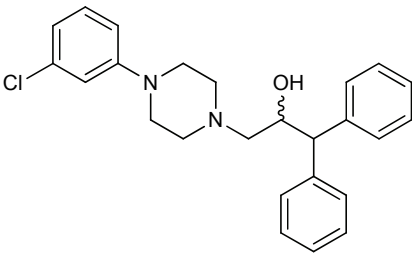
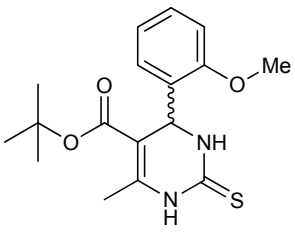
Brian Shoichet: *shoichet@cgl.ucsf.edu*, phone: 415-514-4126, fax: 415-514-4126

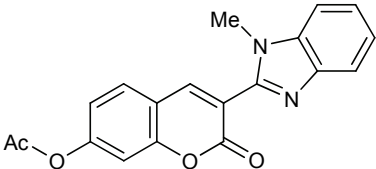
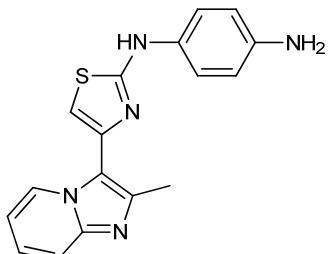
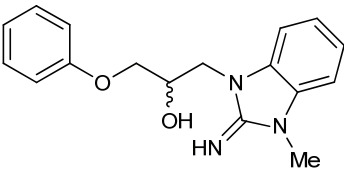
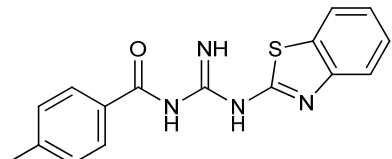
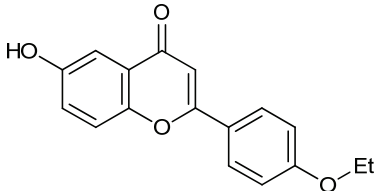
SUPPLEMENTARY RESULTS

Supplementary Table 1 | Representative, high-confidence but untested target predictions for compounds active in the zebrafish screen. Targets across biological categories (i.e., GPCRs, ligand-gated ion channels, transporters, nuclear hormone receptors, enzymes) are predicted.

Compound	Predicted Target	Confidence relative to random (SEA E-value)
 15	PDE1B	7.76×10^{-11}
 16	PDE4A	6.52×10^{-65}
 17 (SKF-82958)	adenylate cyclase VII	2.99×10^{-57}
 18 (A-77636)	adenylate cyclase IX	6.38×10^{-44}

	malic enzyme 1	2.52×10^{-60}
19		
	$\Delta 8$ - $\Delta 7$ sterol isomerase	3.23×10^{-15}
20		
	sirtuin 1	1.00×10^{-12}
21		
	Na/K-transporting ATPase	1.54×10^{-23}
22 (strophanthidinic acid lactone acetate)		

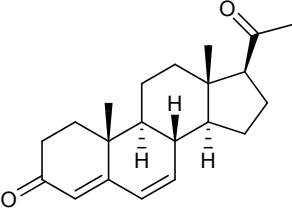
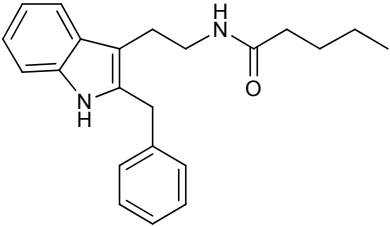
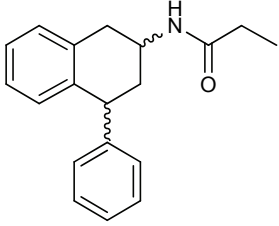
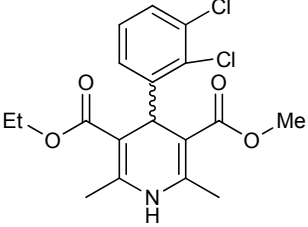
	NADH-ubiquinone oxidoreductase	5.89×10^{-56}
23 (β -toxicarol)		
	acetylcholinesterase MCH receptor 1	1.55×10^{-94} 1.37×10^{-45}
24 (4-IBP)		
	pancreatic alpha-amylase M4 muscarinic receptor	1.62×10^{-70} (FCFP4) 2.08×10^{-17} (FCFP4)
25 (PRE-084)		
	glycine transporter 1	1.26×10^{-51}
26		
	vesicular acetylcholine transporter	2.10×10^{-10}
27 (BRL 15572)		
	fatty acid transport protein 4	8.15×10^{-30}
28		

	macrophage migration inhibitory factor	4.84×10^{-18}
29		
	tubulin	1.92×10^{-43}
30		
	Nav1.1	2.87×10^{-14}
31		
	Nav1.5	2.01×10^{-21}
32		
	GABA-A	4.16×10^{-10} (FCFP4)
33		

	5-HT3B	1.34×10^{-21}
34		
	adenosine A1 receptor	2.34×10^{-21}
35		
	vanilloid receptor 1	9.07×10^{-11}
36		
	mGluR5	5.83×10^{-11}
37		
	progesterone receptor	6.73×10^{-30}
38		

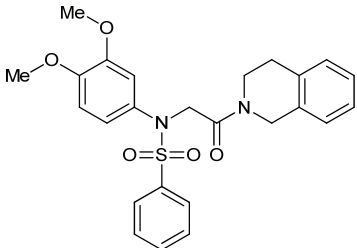
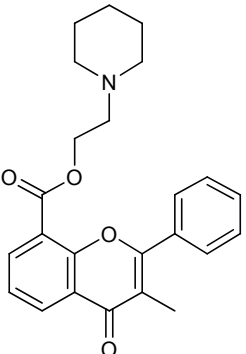
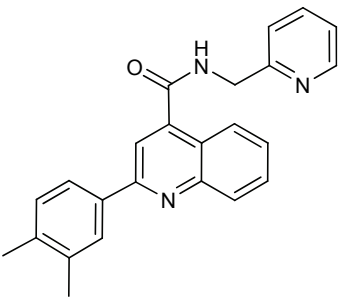
	nociceptin receptor	2.14×10^{-34}
39		
	nociceptin receptor	1.99×10^{-41}
40 (fluspirilene)		
	κ opioid	3.76×10^{-12}
41		
	dopamine D3	7.75×10^{-26}
42		

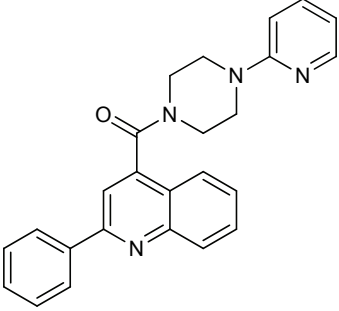
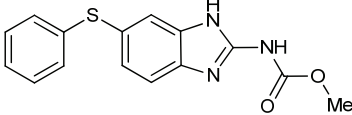
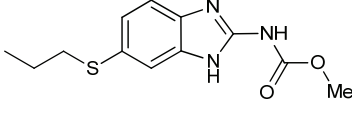
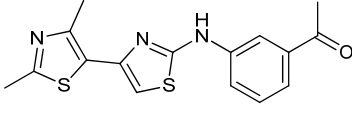
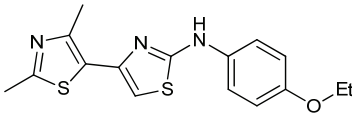
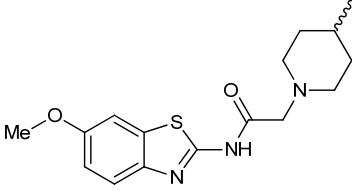
Supplementary Table 2 | Compound-target predictions that, though not in our databases, could be verified by literature search.

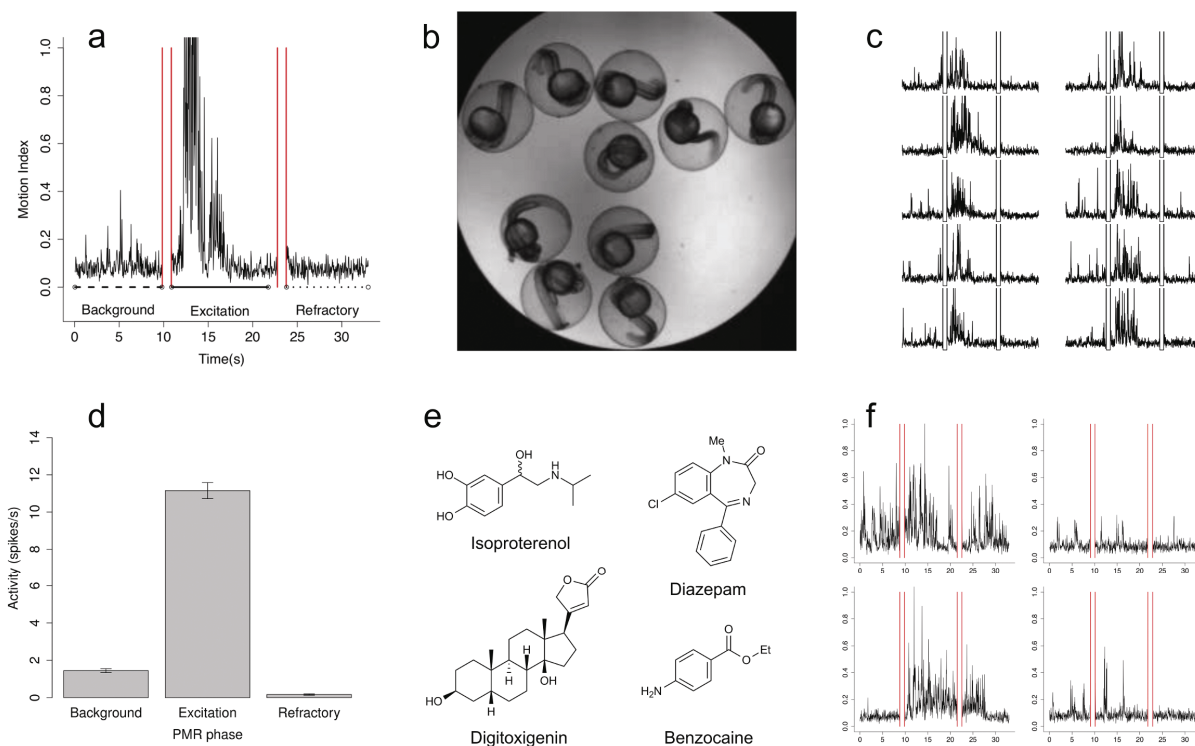
Compound	Predicted Target	Confidence relative to random (SEA E-value)
 43 (progesterone)	CYP17a	1.5710^{-15}
 44	melatonin MT ₃ ¹ melatonin MT ₁ ¹ melatonin MT ₂ ¹	3.78×10^{-60} 3.78×10^{-60} 7.97×10^{-58}
 45	melatonin MT ₂ ² melatonin MT ₁ ²	3.54×10^{-15} 8.66×10^{-15}
 46 (felodipine)	voltage-dependent L-type calcium channel Cav1.2 ³	8.22×10^{-26}

	5-HT1A ⁴	1.52×10^{-96}
<p>47 (5-methylurapidil)</p>		
	histamine N-methyltransferase (HMT) ⁵	1.36×10^{-54}
<p>48 (zolantidine)</p>		
	5-HT1A ⁶	2.92×10^{-31}
<p>49</p>		
	dopamine D1 ⁷	8.65×10^{-20}
<p>50 (CY 208-243)</p>		
	carbonate dehydratase IV ⁸	4.16×10^{-10} (FCFP4)
<p>51 (trichlormethiazide)</p>		

Supplementary Table 3 | Tested compounds that failed to show activity on the predicted molecular target.

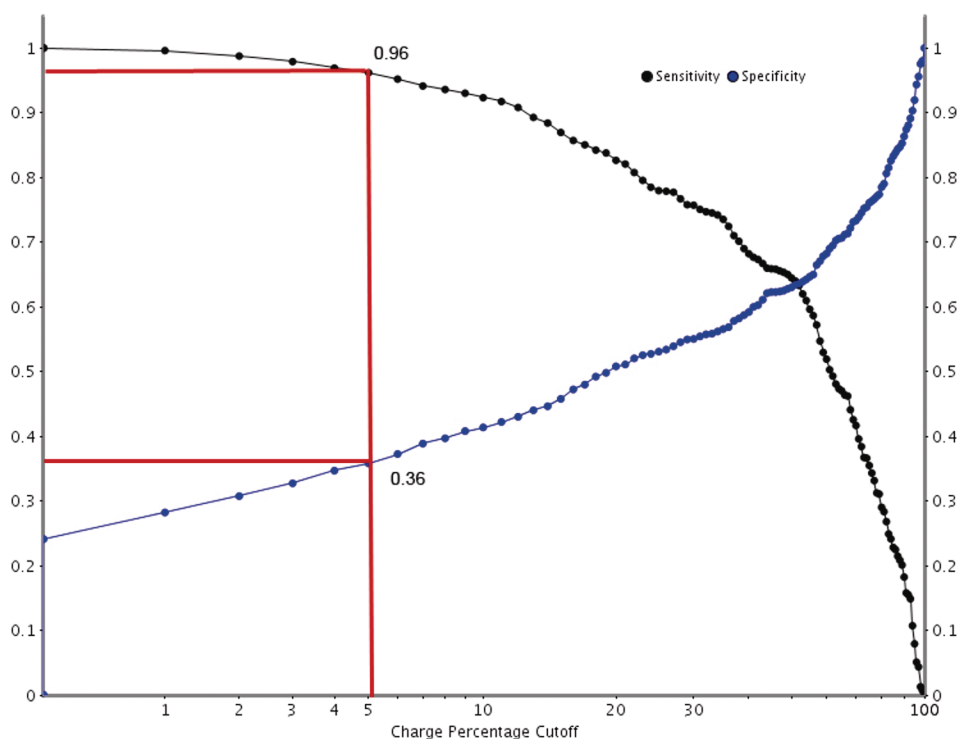
Compound	Predicted targets	E-value	K _i (nM)
 <p>52</p>	oxytocin	1.49×10^{-27}	> 10,000
	vasopressin 1A	1.22×10^{-07}	> 10,000
 <p>53 (flavoxate)</p>	5-HT ₄	1.50×10^{-23}	> 10,000
	 <p>54</p>	NK3	8.54×10^{-96}

 <p>55</p>	NK3	2.38×10^{-67}	Agonist 3.1% Antagonist 0.8%
 <p>56 (fenbendazole)</p>	TIE-2	3.46×10^{-18}	> 10,000
 <p>57 (albendazole)</p>	TIE-2	7.53×10^{-18}	> 10,000
 <p>58</p>	CDK7 CDK9	1.92×10^{-13} 7.19×10^{-13}	> 10,000 > 10,000
 <p>59</p>	CDK4 CDK7 CDK9 Aurora-A Aurora-B	1.53×10^{-7} 2.19×10^{-23} 1.54×10^{-18} 4.69×10^{-5} 3.88×10^{-8}	> 10,000 > 10,000 > 10,000 > 10,000 > 10,000
 <p>60</p>	LCK	1.01×10^{-14}	> 10,000

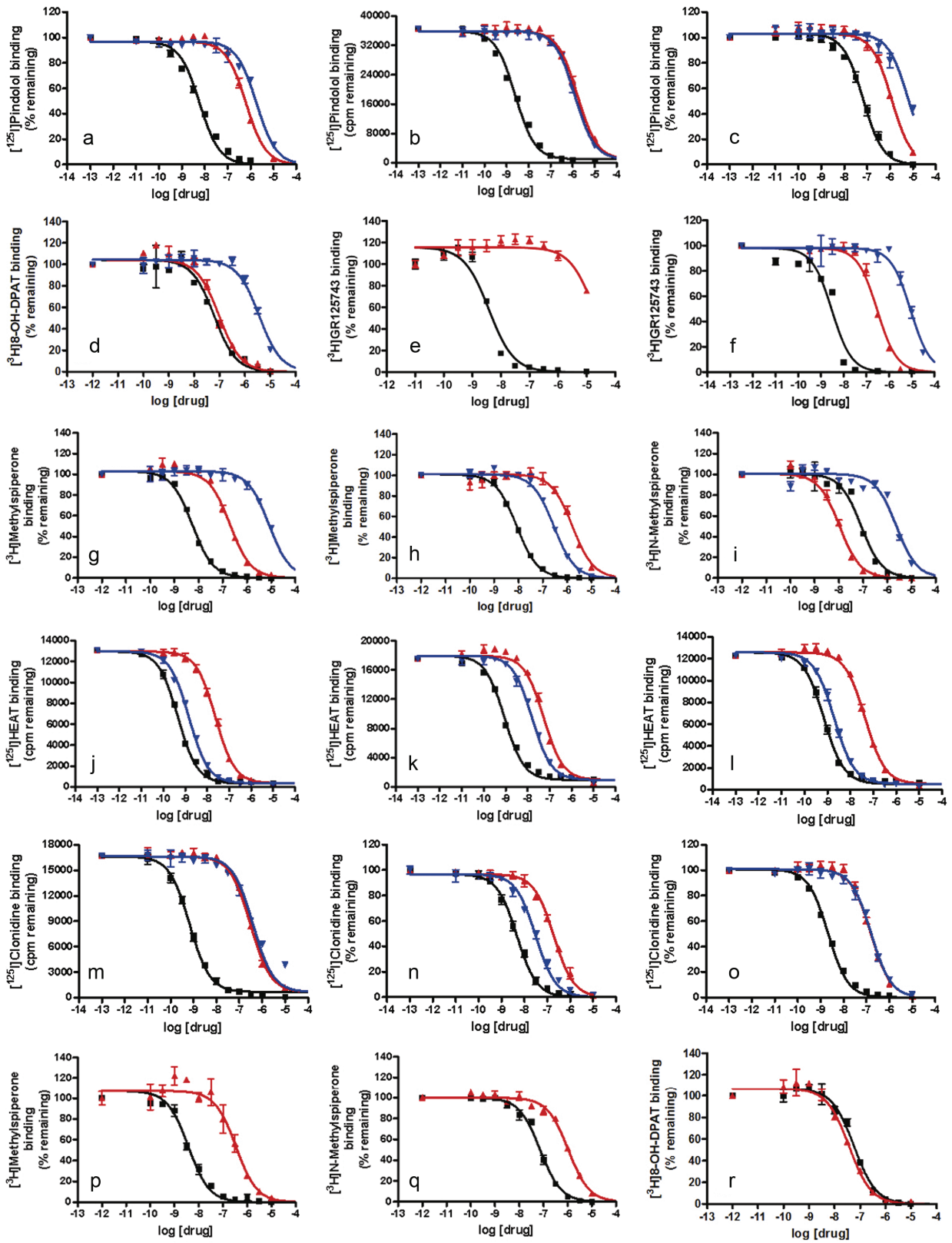


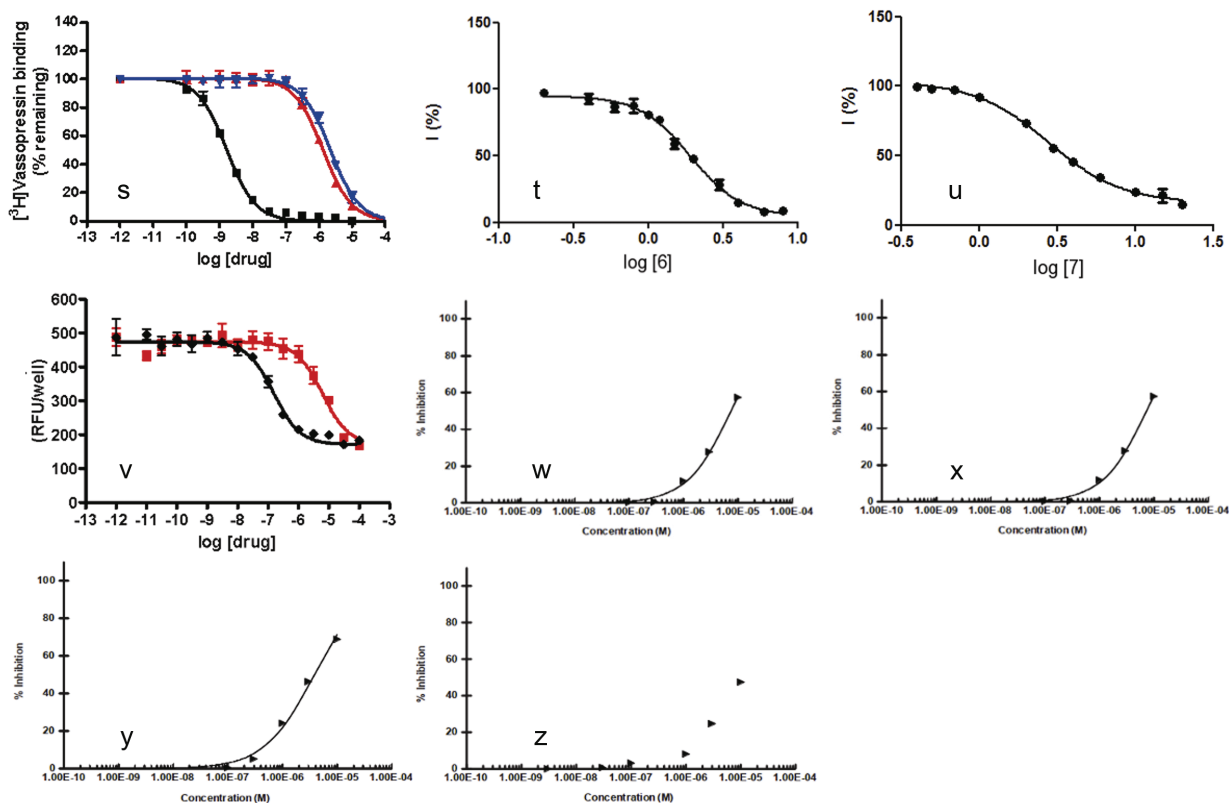
Supplementary Figure 1 | The PMR is a behavior-based HTS screening assay in zebrafish.

(a) The aggregate motor activity of 10 zebrafish embryos during the PMR assay. The y-axis and x-axis represent the motion index and time, respectively. Red vertical bars at 10s and 23s represent the timing and duration of the stimulus. Dashed, solid and dotted lines indicate the PMR background, excitation and refractory phases. (b) Image of 10 zebrafish embryos in a single well of a 96-well plate. (c) Plots from ten independent control wells during the PMR assay. (d) Bar plot showing the mean number \pm s.d. of motor activity spikes/s during the indicated PMR phase. (e) Four representative drugs that exhibit a specific PMR response. (f) Plots showing the motor activity of animals in wells treated with the compounds indicated in panel e.



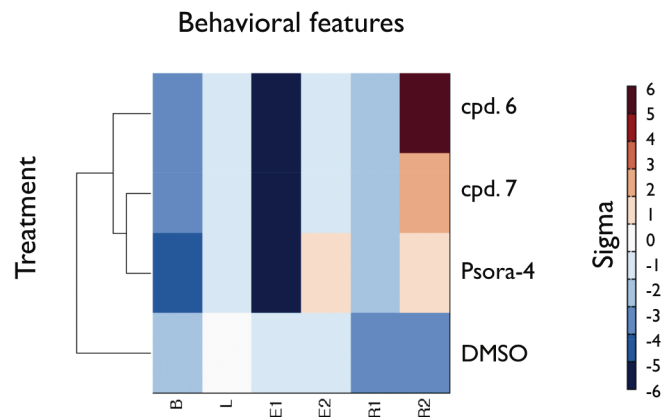
Supplementary Figure 2 | Use of a post-SEA charge filter to remove predictions that did not have the same charge as the majority of annotated ligands. In retrospective calculations, on known ligand-target annotations from the reference ChEMBL database, we investigated how stringent a charge filter we could use to maximize our sensitivity (Se) and specificity (Sp). The marked points corresponds to a cutoff value of 5%, at which $Se=0.96$ and $Sp=0.36$, which was selected for filtering the predictions. The biggest improvement step in Sp was reached by just requiring that the predicted protonation state of the candidate molecule was reflected by at least one molecule in the target set (Charge percentage > 0%). Even at low cutoff values we begin to lose some of the true actives, as can be seen in the decline of Se .





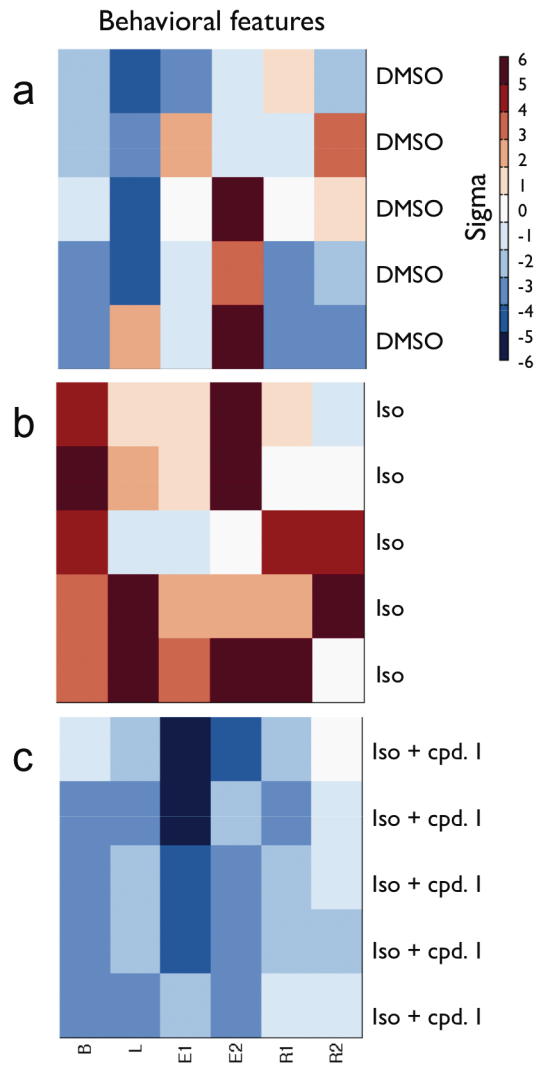
Supplementary Figure 3 | Concentration-response curves for all active molecules on their predicted targets.

The black curves in A-S and V are those of reference compounds that were measured together with our compounds. For K_i and IC_{50} values see **Table 1**. Concentration values on the x-axis of T and U are given as log micromolar. Cpd. 5 was also assayed at $\alpha_{1A,B,D}ARs$, $\alpha_{2A,B,C}ARs$, and $5HT_{1A}$ – these targets were predicted, but found out later to be known.⁹⁻¹¹ In our hands, affinities of cpd. 5 at these targets were 0.8, 8.7, 1.1, 213.8, 15.7, 80.8, and 25.0 nM, respectively. (a) β_1AR , cpd. 1 (red), 2 (blue). (b) β_2AR , cpd. 1 (red), 2 (blue). (c) β_3AR , cpd. 1 (red), 2 (blue). (d) $5-HT_{1A}$, cpd. 3 (red), 4 (blue). (e) $5-HT_{1B}$, cpd. 3 (red). (f) $5-HT_{1D}$, cpd. 3 (red), 4 (blue). (g) dopamine D_2 , cpd. 3 (red), 4 (blue). (h) dopamine D_3 , cpd. 4 (red), 5 (blue). (i) dopamine D_4 , cpd. 3 (red), 4 (blue). (j) $\alpha_{1A}AR$, cpd. 3 (red), 5 (blue). (k) $\alpha_{1B}AR$, cpd. 3 (red), 5 (blue). (l) $\alpha_{1D}AR$, cpd. 3 (red), 5 (blue). (m) $\alpha_{2A}AR$, cpd. 3 (red), 5 (blue). (n) $\alpha_{2B}AR$, cpd. 3 (red), 5 (blue). (o) $\alpha_{2C}AR$, cpd. 3 (red), 5 (blue). (p) dopamine D_2 , cpd. 5 (red). (q) dopamine D_4 , cpd. 5 (red). (r) $5-HT_{1A}$, cpd. 5 (red). (s) vasopressin V_{1A} , cpd. 8 (red). (t) $Kv1.2$, cpd. 6. (u) $Kv1.2$, cpd. 7. (v) SERT, cpd. 9 (red). (w) ABL2, cpd. 10. (x) SRC, cpd. 10. (y) LCK,

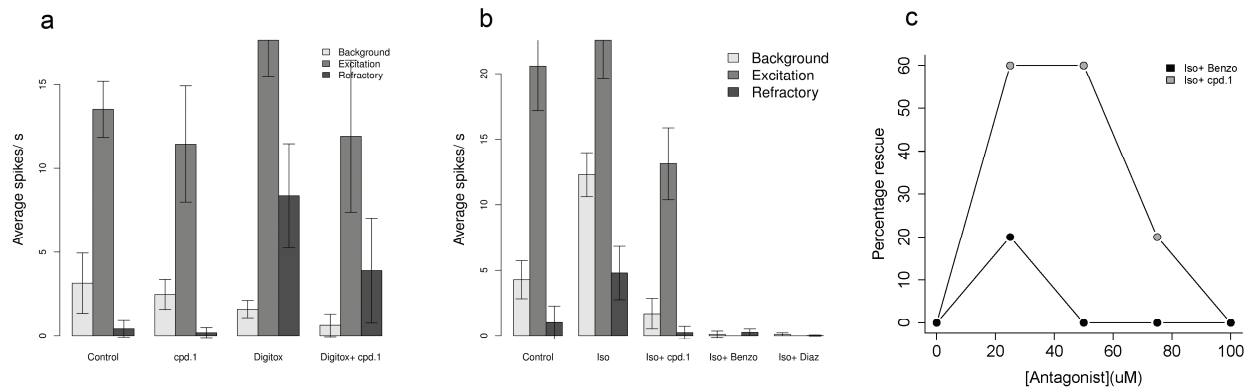


cpd. 10. (z) p38 α , cpd. 11.

Supplementary Figure 4 | Compound 12 phenocopies compounds 6 and 7. Dendrogram and heatmap showing hierarchical clustering of behavioral profiles from wells treated with DMSO, compound 12 (psora-4), compound 6, or compound 7. Colorbar shows the range of sigma values displayed in the heatmap.



Supplementary Figure 5 | Compound 1 normalizes isoproterenol (compound 13)-induced behavioral stimulation. Heatmaps showing behavioral profiles from multiple wells treated with (a) DMSO, (b) compound 13 (Iso), or (c) compounds 13 + 1. The colorbar shows the range of sigma values displayed in the heatmap.



Supplementary Figure 6 | The predicted beta antagonist compound 1 shows specific interactions with compound 13 (isoproterenol). (a) Compound 1 does not rescue the stimulating effects of the Na^+/K^+ ATP-ase blocker digitoxigenin. Bar plot showing the mean number of motor activity spikes/s in animals treated with the indicated compounds. (b) Compound 1, but not the Na^+ channel blocker benzocaine, nor the GABA-A agonist diazepam, rescues the stimulating effects of 13. (c) Line chart showing the percentage of animals rescued by the indicated treatments. See also **Supplementary Fig. 1** for the PMR plots of 13, digitoxigenin, benzocaine, and diazepam.

SUPPLEMENTARY METHODS

Zebrafish behavioral pharmacology. Embryos were collected from group matings of Ekwill or TuAB zebrafish and raised in HEPES (10 mM) buffered E3 media in a dark 28 °C incubator. At 28 hpf, groups of 8-10 embryos were distributed into the wells of a 96 well plate. Compound stocks were diluted into each well at the specified concentration and allowed to incubate for 1 hour.

To assay the PMR, 1000 frames of digital video were recorded at 33fps using a Hamamatsu ORCA-ER camera attached to a Nikon TE200 microscope at 1X magnification. Light stimuli (1s)—from a 300Watt xenon bulb housed in a Sutter Lambda LS illuminator— were delivered 10s and 20s after the start of the video. Instrument control and data measurement were performed using custom programs for Metamorph Software (Universal Imaging). Each video was saved for review.

To analyze digital video recordings, custom software scripts (Metamorph) were used to automatically draw six evenly spaced line segments across the well such that each embryo is likely to be crossed by one of the lines. The software then tracks the average intensity of the pixels for each segment over time. Embryo movement changes the light intensity at some pixels, leading to a commensurate change in the average intensity of the affected lines. A motion index was formed by taking the absolute value of the difference in average pixel intensity for adjacent time points and then summing over the six segments. This motion index correlates with the overall amount of motion in the well, both in terms of contraction frequency and number of animals in motion. The value of this motion index over time constitutes the basic behavioral phenotype. The motion index profile for each well was partitioned into three periods— background, excitation and refractory— based on the following landmarks: Background = start to pulse 1, Excitation = pulse 1 to pulse 2, refractory = pulse 2 to stop.

To treat zebrafish with chemicals, stock solutions in DMSO were added to each well, mixed, and allowed to incubate for 1h. Final DMSO concentrations were <1%. In experiments with multiple compounds, the compounds were added simultaneously.

Hierarchical clustering of behavioral profiles. For each well, the Motion Index was divided into six behavioral features based on time and representing the PMR background,

latency, early excitation, late excitation, early refractory and late refractory phases (B, L, E1, E2, R1, R2). These values were then transformed to the relative number of standard deviations (sigma values) from the control mean for each feature. These six values comprise the behavioral profile. Behavioral profiles were clustered using Euclidean distance and average linkage clustering.

Cheminformatics. We used the similarity ensemble approach (SEA) algorithms to predict candidate molecular targets for every hit compound, using a selection of Scitegic¹² and Daylight¹³ topological fingerprints. SEA relates proteins based on the set-wise chemical similarity of their ligands, or single molecules to target-ligand sets, correcting for the similarity one might expect at random, as previously described.¹⁴⁻¹⁶ A filtered pre-release version of the ChEMBL database (<https://www.ebi.ac.uk/chembl/db/>) provided a reference set of target-annotated compounds. Pipeline Pilot version 6.1.1.0 (Accelrys) provided Scitegic fingerprints and was used to compare some behavioral similarities. For compound clustering we used Cytoscape 2.8 with the Cluster, Cheminformatics, and VistaClara plugins. Charges for the charge-filtering protocol were computed with Epik 2.1107 (Schrödinger), and chemical structures were drawn with ChemDraw 12.0.

Clustering of hits by chemical and phenotypic similarity. Chemical and phenotypic similarities were computed with Pipeline Pilot as Tanimoto values based on ECFP4 fingerprints and Euclidean distance values based on the behavioral σ values for the different time slots, respectively. Chemical distances above 0.72 and behavioral distances above 0.4 were discarded. The compounds, their phenotypic profiles and remaining pairwise distance values were imported into Cytoscape and clustered with Markov (MCL) and Transitivity Clustering methods using chemical similarities. Several interesting clusters of compounds sharing both chemical and behavioral similarities emerged, which helped us in prioritizing compounds that were inspected for their predicted targets.

Target prediction using SEA. For each compound active in the behavioral screen, possible targets were calculated with SEA, using Scitegic ECFP4, ECFP6, FCFP4, and FCFP6,¹² as well as Daylight fingerprints¹³ with the widely used Tanimoto coefficient (T_C)¹⁷ as similarity metric. Unless otherwise noted, numbers in the manuscript are given for the ECFP4 results. The ChEMBL database (<https://www.ebi.ac.uk/chembl/db/>) was filtered for compounds annotated for protein targets with affinity values below 10 μ M and at least five molecules

annotated for each target. Only compound-target predictions that were not already known in ChEMBL were considered. Initial predictions were filtered with a charge-filter protocol: for a given target, all protonation states with a better than a 1% likelihood were calculated for each target compound at pH 6-8. The most likely protonation state at pH 6-8 of predicted compounds also was calculated. A compound-target prediction was only kept if the primary protonation state of the candidate molecule was represented in at least 5% of the target set compounds (**Supplementary Fig. 2**). As an additional guide during visual inspection, targets were annotated with biological process information from the Gene Ontology (GO) database (<http://www.geneontology.org>) and pathway information from the Reactome database (<http://www.reactome.org>).

Ligands selected for target identification. Selected hits from our SEA prediction that passed a visual inspection and had testable targets were sourced from the following commercial vendors: compounds **1, 3, 4, 6-8, 10, 11,** and **52, 54, 55, 58,** and **60** were ordered from ChemBridge, compound **2** from Life Chemicals, compound **5** from Tocris, compounds **9, 56,** and **57** from Sigma-Aldrich, compound **53** from MP Biomedicals, and compound **59** from Otava Chemicals. All compounds were sourced at 95% or greater purity as described by the vendors. All active compounds were further tested at UCSF for purity by LC/MS, and all were found to be pure as judged by peak height and identity. For the phenocopy and phenotype inversion experiments, compounds **12** and **13** were sourced from Sigma-Aldrich and compound **14** from Enzo Life Sciences, at 98% or greater purity grades.

Radioligand competition binding assays of compounds 1-5, 8, 52 and 53. Crude P2 (21,000 x g) membrane preparations were prepared from cell lines expressing (either stably or transiently) recombinant human GPCRs using 50 mM Tris, 1% BSA, pH 7.4 at a concentration of ca. 50 μg protein/ μL (assayed by Bradford assay using BSA as a standard). Next, 50 μL of membrane suspension were added to the wells of a 96-well plate containing 100 μL of binding assay buffer, 50 μL of radioligand at a concentration equal to five times the dissociation constant (K_d) for the receptor being assayed, and 50 μL of test drug or reference compound at a concentration equal to five times the desired assay concentration (**Supplementary Table 4**). Reactions were incubated for 60 to 90 min at room temperature in the dark, and then harvested onto 0.3% PEI-treated GF/A filtermats (Wallac). After three washes with ice-cold wash buffer (50 mM Tris, pH 7.4), filter mats were dried in a microwave oven and impregnated with Meltilex scintillant (Wallac). Residual binding of radioligand, measured by scintillation counting using a

TriLux microbeta counter (Wallac), was fit to the one-site radioligand competition binding model (i.e., a three-parameter logistic equation) in Prism 4.0 (GraphPad) to obtain log IC₅₀ values. Affinity constants (K_i values) were calculated from best-fit IC₅₀ values using the Cheng-Prusoff approximation.

Functional Agonist/Antagonist Assays of compounds 54 and 55. HEK293 cells stably expressing recombinant human NK3 receptors were plated in poly-L-lysine-coated 384-well plates at a density of 20,000 cells per well in DMEM containing 1% dialyzed fetal bovine serum. The next day, the cell culture media was replaced with 20 µl/well of HBSS, 20 mM HEPES, 2.5 mM probenecid, pH 7.4 (assay buffer) containing 1X Fluo4 direct calcium assay reagent (Invitrogen). After a one-hour incubation at 37°C, the plates were loaded into a FLIPR Tetra (MDS) and the baseline fluorescence was read for 10 sec (1 read/sec). To measure agonist activity, the cells were stimulated with 10 µL of 3X test drug or reference compound (substance P) prepared in assay buffer, and calcium responses (fold over baseline) were recorded for 180 sec (1 read/sec). To assess antagonist activity, the cells were treated with test compound or buffer and incubated for 6 min, after which the cells were challenged with agonist (substance P) at a concentration equal to the EC₉₀ at the receptor being assayed.

Electrophysiological studies of compounds 6 and 7. For these recordings, 10ng of rat Kv1.2 mRNA (T7 mMessenger, Ambion) were microinjected into defolliculated stage V-VI *Xenopus laevis* oocytes.¹⁸ Two-electrode voltage clamp recordings were performed 24 hours post-injection in a bath of 90K solution (90 mM KCl, 2.0 mM MgCl₂, 10mM HEPES pH 7.5) using standard microelectrodes (0.3 to 3 MΩ) filled with 3M KCl. Currents were recorded using a GeneClamp 500B amplifier (Axon Instruments) controlled by a 1200 MHz processor computer (Celeron Gateway) running CLAMPEX 8.2.0.244. Currents were digitized at 1 kHz with Digidata 1332A (Axon Instruments) and analyzed with Clampfit 8.2 (Axon Instruments). To generate concentration-response curves, membrane potential was held at -80mV and depolarized from -100 to +30mV in 10mV steps, followed by a tail current command of -80mV. Current amplitudes were compared at +30mV after application of various compound concentrations for 1300msec, and the data were fitted using the Hill equation: $I = I_{\min} + (I_{\max} - I_{\min}) / [1 + ([\text{inh}] / IC_{50})^H]$, where I is the percentage of remaining current in the presence of the inhibitor, I_{max} and I_{min} are maximal and minimal current values respectively, [inh] represents the inhibitor concentration and H is the Hill coefficient. Each data point represents the mean of four to seven independent measurements and error bars indicate SEM.

Inhibition of SERT uptake by compound 9. Substrate uptake into HEK-SERT cells treated with vehicle, compound **9**, or reference compounds was assessed using the Molecular Devices Transporter Explorer Kit following the manufacturer's protocol. Compound **9** inhibited substrate uptake by HEK-SERT cells with a potency similar to that of cocaine. HEK cells not expressing SERT exhibited no specific substrate uptake (i.e., fluorescence values were comparable to those observed in HEK-SERT cells treated with 10 μ M fluoxetine). Furthermore, compound **9** exhibited an $IC_{50} > 10 \mu$ M for substrate uptake by HEK-DAT cells, suggesting that the effect seen in HEK-SERT cells reflects compound activity at SERT itself and not modulation of some other component of transporter activity (e.g., ion gradients, ATP, etc.).

Off-chip Mobility Shift Assay (MSA) for compounds 10, 11, and 56-60. Assays were performed by CarnaBio using the following procedure: The 5 μ L of x4 compound solution, 5 μ L of x4 substrate/ATP/Metal solution, and 10 μ L of x2 kinase solution were prepared with assay buffer (20 mM HEPES, 0.01% Triton X-100, 2 mM DTT, pH7.5) and mixed and incubated in a well of a polypropylene 384 well microplate for 1 or 5 hours at room temperature (depending on the kinase). To stop the reactions, 60 μ L of Termination Buffer (QuickScout Screening Assist MSA; Carna Biosciences) were added to the well. The reaction mixture was applied to a LabChip3000 system (Caliper Life Science), and the product and substrate peptide peaks were separated and quantitated. Substrate-to-product conversion was calculated from the peak heights of the product(P) and substrate(S) peptides as $P/(P+S)$. Detailed reaction conditions are given in **Supplementary Table 5**.

Supplementary Table 4 | Assay conditions for GPCR radioligand competition binding assays.

Receptor	Binding Assay Buffer	Reference	Radioligand
α_{1A}	20 mM Tris, 145 mM NaCl, pH 7.4	Prazosin	[¹²⁵ I]HEAT
α_{1B}	20 mM Tris, 145 mM NaCl, pH 7.4	Prazosin	[¹²⁵ I]HEAT
α_{1D}	20 mM Tris, 145 mM NaCl, pH 7.4	Prazosin	[¹²⁵ I]HEAT
α_{2A}	50 mM Tris, 5 mM MgCl ₂ , pH 7.7	Prazosin	[¹²⁵ I]Clonidine
α_{2B}	50 mM Tris, 5 mM MgCl ₂ , pH 7.7	Prazosin	[¹²⁵ I]Clonidine
α_{2C}	50 mM Tris, 5 mM MgCl ₂ , pH 7.7	Prazosin	[¹²⁵ I]Clonidine
β_1	50 mM Tris, 3 mM MnCl ₂ , pH 7.7	Alprenolol	[¹²⁵ I]Pindolol
β_2	50 mM Tris, 3 mM MnCl ₂ , pH 7.7	Alprenolol	[¹²⁵ I]Pindolol
β_3	50 mM Tris, 3 mM MnCl ₂ , pH 7.7	Alprenolol	[¹²⁵ I]Pindolol
D ₂	20 mM HEPES, 100 mM NMDG, 10 mM MgCl ₂ , 1 mM EDTA, 1 mM EGTA, pH 7.4	Haloperidol	[³ H] <i>N</i> -methylspiperone
D ₃	20 mM HEPES, 100 mM NMDG, 10 mM MgCl ₂ , 1 mM EDTA, 1 mM EGTA, pH 7.4	Chlorpromazine	[³ H] <i>N</i> -methylspiperone
D ₄	20 mM HEPES, 100 mM NMDG, 10 mM MgCl ₂ , 1 mM EDTA, 1 mM EGTA, pH 7.4	Chlorpromazine	[³ H] <i>N</i> -methylspiperone
5-HT _{1A}	50 mM Tris, 10 mM MgCl ₂ , 0.1 mM EDTA, pH 7.4	Methysergide	[³ H]8-OH-DPAT
5-HT _{1B}	50 mM Tris, 10 mM MgCl ₂ , 0.1 mM EDTA, pH 7.4	Ergotamine	[³ H]5-CT
5-HT _{1D}	50 mM Tris, 10 mM MgCl ₂ , 0.1 mM EDTA, pH 7.4	Ergotamine	[³ H]5-CT
5-HT ₄	50 mM Tris, 10 mM MgCl ₂ , 0.1 mM EDTA, pH 7.4	GR113808	[³ H]GR113808

OT	20 mM Tris, 100 mM NaCl, 10 mM MgCl ₂ , 0.1 mg/ml bacitracin, 1 mg/ml BSA, pH 7.4	Oxytocin	[³ H]Oxytocin
V _{1A}	20 mM Tris, 100 mM NaCl, 10 mM MgCl ₂ , 0.1 mg/ml bacitracin, 1 mg/ml BSA, pH 7.4	Arg- Vasopressin	[³ H]Arg- Vasopressin

Supplementary Table 5 | Assay conditions for kinase mobility shift assays.

Kinase	Substrate		ATP (μM)		Metal		Positive control	Reaction time (hr)
	Name	(nM)	Km	Assay	Name	(mM)		
ARG (ABL2)	ABLtide	1000	24	25	Mg	5	Staurosporine	1
LCK	Srctide	1000	14	10	Mg	5	Staurosporine	1
SRC	Srctide	1000	31	50	Mg	5	Staurosporine	1
TIE2	Blk/Lyntide	1000	94	100	Mg	5	Staurosporine	1
AurA	Kemptide	1000	27	25	Mg	5	Staurosporine	1
AurB/INCENP	Kemptide	1000	16	25	Mg	5	Staurosporine	1
CDK4/CycD3	DYRKtide-F	1000	200	200	Mg	5	Staurosporine	5
CDK7/CycH/MAT1	CTD3 peptide	1000	32	50	Mg	5	Staurosporine	5
CDK9/CycT1	CDK9 substrate	1000	9.4	10	Mg	5	Staurosporine	5
p38α	Modified Erktide	1000	150	150	Mg	5	SB202190	1

SUPPLEMENTARY REFERENCES

1. Teh, M.T. & Sugden, D. *Naunyn Schmiedebergs Arch. Pharmacol.* **358**, 522-8 (1998).
2. Durieux, S. et al. *Bioorg. Med. Chem.* **17**, 2963-74 (2009).
3. Cohen, C.J., Spires, S. & Van Skiver, D. *J. Gen. Physiol.* **100**, 703-28 (1992).
4. Gross, G., Hanft, G. & Kolassa, N. *Naunyn Schmiedebergs Arch. Pharmacol.* **336**, 597-601 (1987).
5. Dyson, H.J., Rance, M., Houghton, R.A., Lerner, R.A. & Wright, P.E. *J. Mol. Biol.* **201**, 161-200 (1988).
6. Barton, A.C. et al. *Brain Res.* **547**, 199-207 (1991).
7. Markstein, R. et al. in *Progress in Catecholamine Research, Part B: Central Aspects*, Vol. Neurology and Neurobiology 42B (eds. Sandler, M., Dahlstrom, A. & Belmaker, R.H.) 59-64 (Alan Liss, New York, 1988).
8. Temperini, C., Cecchi, A., Scozzafava, A. & Supuran, C.T. *Bioorg. Med. Chem.* **17**, 1214-21 (2009).
9. Montorsi, M., Menziani, M.C., Cocchi, M., Fanelli, F. & De Benedetti, P.G. *Methods* **14**, 239-54 (1998).
10. Blaxall, H.S., Murphy, T.J., Baker, J.C., Ray, C. & Bylund, D.B. *J. Pharmacol. Exp. Ther.* **259**, 323-9 (1991).
11. Meana, J.J., Callado, L.F., Pazos, A., Grijalba, B. & Garcia-Sevilla, J.A. *Eur. J. Pharmacol.* **312**, 385-8 (1996).
12. Rogers, D. & Hahn, M. *J. Chem. Inf. Model.* **50**, 742-54 (2010).
13. James, C., Weininger, D. & Delany, J. *Daylight Theory Manual* (Daylight Chemical Information Systems Inc., Aliso Viejo, CA, 1992–2008).
14. Keiser, M.J. et al. *Nat. Biotechnol.* **25**, 197-206 (2007).
15. Hert, J., Keiser, M.J., Irwin, J.J., Oprea, T.I. & Shoichet, B.K. *J. Chem. Inf. Model.* **48**, 755-65 (2008).
16. Keiser, M.J. et al. *Nature* **462**, 175-81 (2009).
17. Willett, P., Barnard, J.M. & Downs, G.M. *J. Chem. Inf. Comput. Sci.* **38**, 983-996 (1998).
18. Minor, D.L. et al. *Cell* **102**, 657-70 (2000).